

# Models for Electrical Signaling in Neurons

Zachary J. McNulty    Ginoveva Ilieva

August 2018

## Abstract

In this paper we motivate two models for the electrical response of a neuron: the Hodgkin-Huxley model and the Fitzhugh-Nagumo model. We first investigate the Hodgkin-Huxley model by generating solutions under standard conditions and analyze them individually. Since the complexity of the Hodgkin-Huxley model makes it difficult to analyze solutions analytically, we then present the simplifications needed to obtain the Fitzhugh-Nagumo model. Computationally, we were able to verify that both systems exhibit the general desired behavior of the biological system: an apparent threshold and oscillatory behavior.

**All code and files used in this paper can be found at: [https://github.com/ig95/project\\_383](https://github.com/ig95/project_383)**

## Introduction

Neurons are the fundamental building blocks of our nervous system, forming complex networks that allow our bodies to perceive, make sense of, and interact with the world around us. Before these networks can be fully understood, it is necessary to understand the individual neurons from which they are constructed. One of the most fundamental activities of a neuron is the *transmission of an electrical signal* along the axon. This process involves a complex interaction between ions such as  $Na^+$  (Sodium) and  $K^+$  (potassium), which are transporting proteins embedded in the membrane of the axon, a varying voltage across the membrane, and the electrical/chemical driving forces that influence the movement and activity of these molecules. As some of these components are *probabilistic*, a full-scale simulation is unrealistic if one hopes to incorporate such a model into a larger network, just due to the sheer number of these components. To give some perspective, a typical neuron can have around 14,000 gated-ion channels, and the human brain has around 100 billion neurons in it [4]. As a result, it is necessary to develop mathematical models that condense this behavior into mathematical systems, which are easier to analyze and manipulate.

## Background Information

### A Brief Summary of the Biology of a Neuron: The Action Potential

The main part of a neuron down which an electrical signal passes is a long, narrow, tubular, and practically empty section called the axon. This axon is sealed off from the fluid surrounding the cell. As such molecules, especially ions, have difficulty entering the cell. Rather, to help facilitate the movement of these ions, there are specialized transport/channel proteins embedded in the cell membrane of the axon that allow these ions to flow through them into the axon, Figure 1.

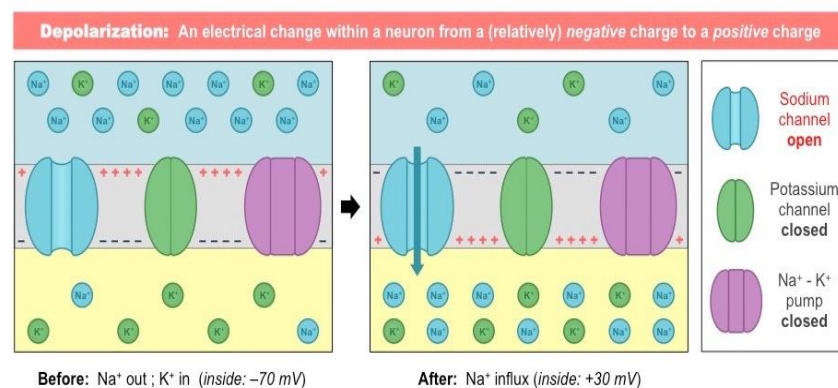


**Fig. 1**

Some of these channels are always open, while some only open under specific conditions, giving the cell some control over its permeability to these ions. In the axon particularly, there are several channel proteins that open in response to changes in the *membrane potential* -- the voltage difference across the axon membrane due to the separation of ions.

There are two main forces acting on these ions: a *concentration gradient*, constantly maintained by ion pumps, and an *electrical/voltage gradient* created by the unequal distribution of charge particles across the membrane. When these channels are open, the ions will flow down these gradients until an electrochemical equilibrium, a balance between the electrical and concentration driving forces, is reached. Electrical signals are passed down the axon through a cascading process called an action potential. During this process, some stimulus, from the outside environment or from a nearby neuron, triggers some of these ion channels to open. As ions flow down their electrochemical gradient into/out of the axon, they change the distribution of charge in nearby regions of the axon. This change creates a change in the membrane potential, which opens or closes nearby ion channels. In doing so, it alters the flow of ions, once more changing the distribution of charge in regions nearby this new segment. As this process continues, this altered charge distribution is passed down along the length of the axon (Fig 2a).

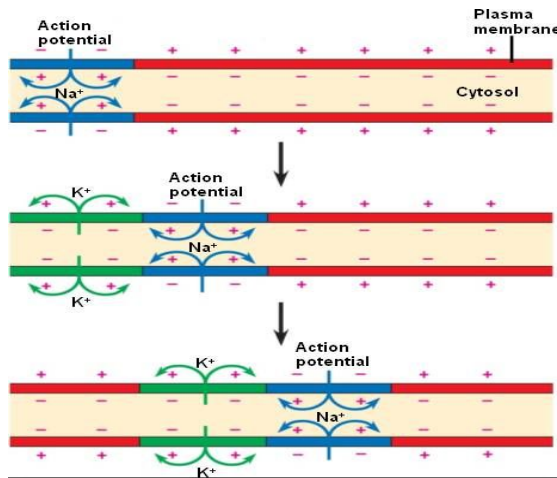


**Fig. 2a**

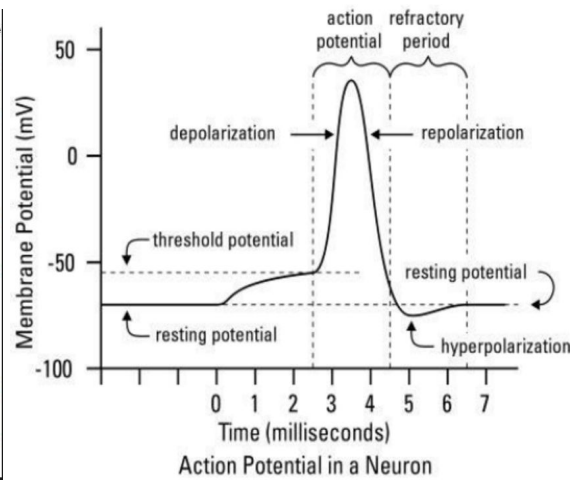


**Fig. 2b**

This is *an action potential*. It is this link between the permeability/conductance of ions and the membrane potential which allows electrical information to be transmitted [1].

More specifically, there exists four main channels involved in this process. *Leaky*  $K^+$  and  $Na^+$  channels ( $L-K^+$  and  $L-Na^+$ ), which are always open, and *voltage-gated*  $K^+$  and  $Na^+$  channels ( $V-K^+$  and  $V-Na^+$ ), which only open once the voltage reaches a certain point. The gradients maintained by the ion pumps will cause  $K^+$  to flow out of the axon, lowering the membrane potential by moving positive charge outward, and  $Na^+$  to flow in, raising the membrane potential. The ion pump and the leaky channels will bring the system back to equilibrium ( $\sim -70$  mV) in response to small perturbations in the membrane potential, but if the potential rises above a certain threshold ( $\sim -55$  mV), the  $V-Na^+$  channels will open and the potential will shoot upwards (these channels far out-number the leaky channels) as  $Na^+$  ions flow into the cell. This period is called depolarization. As the voltage rises,  $V-K^+$  channels begin to open and  $V-Na^+$  begin to close. The process reverses as  $K^+$  flows out of the cell. As the membrane potential drops, all the voltage-gated channels begin to close and the cell once more reaches equilibrium.

## Simplifications

This project will motivate a pre-existing model for the electrical response of a neuron to a given stimuli, the Hodgkin-Huxley (HH) model. This model encapsulates the change in membrane potential and the conductance of ion channels over time as a result of some stimulus. It simplifies the randomness inherent in biological process by forming an analogy between the activity of a neuron and the activity of a circuit. In doing so, it allows us to better characterize this biological system by applying some of the well-understood properties of electrical circuits.

### Equivalent Circuit Model of a Neuron

The model treats each portion of the cell as an electrical element and the circuit is shown in Fig 2. Under this equivalent circuit model, the flow of ions ( $K^+$  and  $Na^+$  mostly) provide a source of output current and the stimulus is some sort of input current. As the electrochemical gradient is the main driving force in this system, it makes sense to model this gradient as the battery which pushes the current along. The impermeable axon membrane provides a source of resistance to the flow of these ions, while the ion channels, both leaky and voltage-gated, provide a source of conductance (although the conductance of the voltage-gated channels is not constant). Lastly, the axon membrane creates a separation of charge due to its impermeability to ions, and thus it naturally acts as a capacitor.

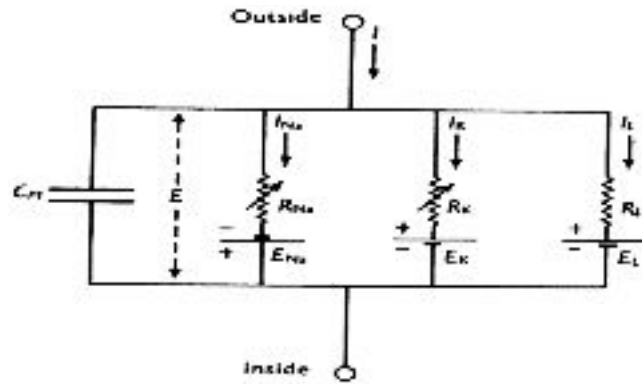


**Fig.3**

Once we have motivated this equivalent circuit model, we can start to develop the model. Due to the conservation of energy/charge, all charge flowing into the system (the input current/stimulus) must either be stored in the capacitor (create a change in membrane potential) or leave the circuit as an output current (ions pass through the membrane). This conservation generates the following equation:

$$C_m \frac{dV_m}{dt} + I_{ion} = I_{ext},$$

**Eqn 1**

where  $C_m$  is the membrane capacitance,  $V_m$  is the membrane potential, and  $I_{ext}$  is the externally applied current. The first term is obtained simply by deriving the capacitance relationship  $q = C_M V_M$  with respect to time, which allows us to consider this charge stored in the capacitor as a current sink.

The ionic current  $I_{ion}$  is the summed result of the flow of  $K^+$  and  $Na^+$  ions through gated and leaky ion channels. In terms of our equivalent circuit, this represents the flow of current

through our conductors. Due to this relationship, we can apply Ohm's law to this circuit element. For example, we can model the current due to  $K^+$  channels as:

$$I = C\Delta V \quad \text{Eqn 2}$$

$$I_K = g_k(t)(V - V_K) \quad \text{Eqn 3}$$

Where  $g_k$  is the time-varying conductance of the  $K^+$  gated ion channel and  $V_K$  is the equilibrium potential of the potassium ions. Applying these to the other ion channels, this allows us to expand equation (1) to the following:

$$I_{ext} = C_m \frac{dV_M}{dt} + g_K(t)(V_M - V_K) + g_{Na}(t)(V_M - V_{Na}) + g_L(V_M - V_L) \quad \text{Eqn 4}$$

Note that the leaky channels are not time-varying: they are always open and thus their conductance is constant.

Lastly, we have to develop a model for these time-varying conductances of the gated channels. Doing so relies on the opening/closing mechanics of these channels. Each of these channels have several gates which physically alter the channel protein. It is these gates that react to changes in voltage, causing a change in the ion permeability. To model the opening and closing of these gates, we will introduce a new equation.

The probability of a gate being open depends on the current value of the membrane voltage. Let  $p_i$  represent the probability a specific gate type  $i$  is open (thus  $0 \leq p_i \leq 1$ ).

$$\frac{dp_i}{dt} = \alpha_i(V)(1 - p_i) - \beta_i(V)p_i,$$

$$\text{Eqn 5, [2]}$$

This equation describes how the proportion of open gates, for a specific gate type, changes over time. Here,  $\alpha$  and  $\beta$  are unique to each type of gate and describe how the activity of that gate changes with respect to time at the current voltage.  $\alpha$  describes how likely a gate is to open, while  $\beta$  describes how likely it is to close. These functions were formulated to match experimental results [2]. In this given system, there are three main gates: a  $K^+$  activation gate, a  $Na^+$  activation gate, and a  $Na^+$  inactivation gate, labeled  $n$ ,  $m$ , and  $h$  respectively. When all activation gates are open, ions can flow through the channel. When just one inactivation gate is closed, ions cannot flow through the channel even if the activation gates are open.  $K^+$  channels are only open if all four of their activation gates are open, and thus the probability such a channel is open is  $n^4$ .  $Na^+$  channels are only open if all 3 of their activation gates are open and if their single inactivation gate is open, and thus the probability such a channel is open is  $m^3h$ .

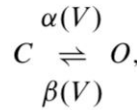
Thus the full conductances with respect to time can be surmised in the following manner:

$$\begin{aligned}
I &= C_m \frac{dV_m}{dt} + \bar{g}_K n^4 (V_m - V_K) + \bar{g}_{Na} m^3 h (V_m - V_{Na}) + \bar{g}_l (V_m - V_l), \\
\frac{dn}{dt} &= \alpha_n(V_m)(1 - n) - \beta_n(V_m)n \\
\frac{dm}{dt} &= \alpha_m(V_m)(1 - m) - \beta_m(V_m)m \\
\frac{dh}{dt} &= \alpha_h(V_m)(1 - h) - \beta_h(V_m)h
\end{aligned}
\tag{Eqn 6, [2]}$$

Here,  $\bar{g}_K, \bar{g}_{Na}, \bar{g}_l$  represent the maximum conductances of their respective channels. Thus, the conductance at any given time is simply a fraction of the maximum, based on the proportion of open channels. This is the full Hodgkin-Huxley model.

#### Analysis of Gating Functions and Gating Variable Behavior:

The conductances of the HH model can be view as a result of combined effects of a large number of ion channels embedded in the membrane. Each individual ion channel can be thought of as containing one or more physical gates that regulate the flow of ions through the channel. Every single gate can be in either permissive or non-permissive state. When all of the gates for a particular channel are in the permissive state, ions can pass through the channel and the channel is open, otherwise when all of the gates are in non-permissive state ions cannot pass and the channel is close. The gate model is summarized by the diagram below [6]



where C = closed and O = open state.  $\alpha(V)$  and  $\beta(V)$  are the voltage-dependent rate constants at which a gate goes from the closed to the open and from the open to the closed states, respectively. Letting m be the fraction of open gates, from the law of mass action we get

$$\frac{dm}{dt} = \alpha(V)(1 - m) - \beta(V)m = (m_\infty(V) - m)/\tau(V),$$

$$m_\infty(V) = \frac{\alpha(V)}{\alpha(V) + \beta(V)} \quad \text{and} \quad \tau(V) = \frac{1}{\alpha(V) + \beta(V)}.$$

**Eqn 7**

This differential equation has already been solved, and the solution starting from  $m(0)$  is

$$m(t) = m_{\infty}(V) + (m(0) - m_{\infty}(V))e^{-t/\tau(V)}.$$

**Eqn 8**

And its solution approaches the steady-state  $m_{\infty}(V)$  at a rate determined by the time constant  $\tau(V)$ .

In the HH model the voltage dependent  $\alpha$  and  $\beta$  were experimentally determined. The probability of opening or closing a channel depends exponentially on the potential, hence

$$\alpha(V) = A_{\alpha} \exp(-B_{\alpha} V) \quad \text{and} \quad \beta(V) = A_{\beta} \exp(-B_{\beta} V).$$

From where it can be obtained that

$$m_{\infty}(V) = \frac{1}{1 + \exp(-(V - V_h)/V_s)},$$

**Eqn 9**

where  $V_h$  and  $V_s$  are constants. The time constant,  $\tau(V)$ , will generally be a skewed bell-shaped function of  $V$  [6].

The rate at which closed gates transition to an open state is governed by a rate constant,  $\alpha$ , which has units of 1/time and is a function of membrane voltage but not of time. The rate at which open gates transition to the closed state is governed by another rate constant,  $\beta$  [8].

If the membrane voltage  $V(m)$  is clamped at some fixed value  $V$ , then the fraction of gates in the permissive state will eventually reach a steady state value given by the following equation:

$$p_{i,t \rightarrow \infty} = \frac{\alpha_i(V)}{\alpha_i(V) + \beta_i(V)}$$

**Eqn 10, [8]**

The plot of the *activation curves*  $n_{\infty}(V)$ ,  $m_{\infty}(V)$ ,  $h_{\infty}(V)$  along with  $\tau_n(V)$ ,  $\tau_m(V)$ ,  $\tau_h(V)$ .

$n_{\infty}$  and  $m_{\infty}$  are increasing functions that approach zero for hyperpolarizing currents and approach 1 for depolarizing currents, and so  $n$  and  $m$  become activated when the membrane is depolarized. On the other hand,  $h_{\infty}(V)$  is a decreasing function, so the  $Na^+$  channels inactivate when the membrane is depolarized. Since  $\tau_m(V)$  smaller than  $\tau_n$  or  $\tau_h$ ,  $Na^+$  channels activate much faster than they inactivate or  $K^+$  channels open, and that agrees with the results on Figure 4.1, which represents the steady-state opening of the gates, and Figure 4.2 is the time constants. [6]

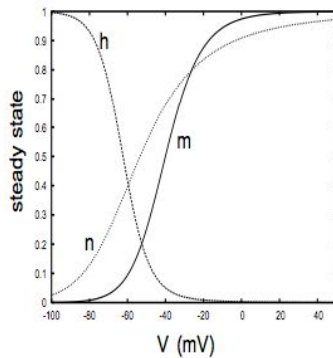


Figure 4.1

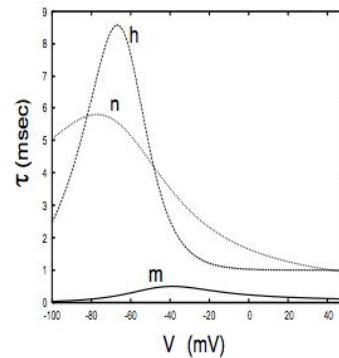


Figure 4.2

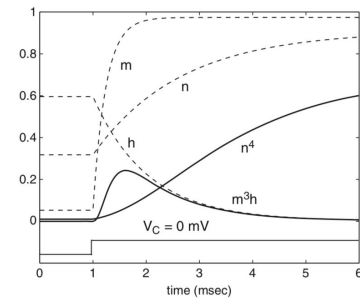


Figure 4.3 [6]

## Computational Analysis of Hodgkin-Huxley Model

Unfortunately, it is difficult to investigate the behavior of solutions to the Hodgkin-Huxley model analytically due to its complexity. Rather, to further investigate the model we will generate some solutions under standard conditions and analyze them individually. Below is a list of the standard parameter values used by Hodgkin and Huxley themselves (approximated experimentally), [1 pg. 520, 2 pg. 32]. This analysis uses the code *HH\_numerical\_integration.m* and the associated function files.

```
% max conductances
g_na = 120;
g_k = 36;
g_l = 0.3;

% Equilibrium Potentials
E_k = -77;
E_na = 50;
E_l = -54.4;

% pg 17 of Foundations of Comp Neuroscience + pg 520 of Hodgkin-Huxley
% paper
c_m = 1;
```

The only parameter left undefined is  $I_{ext}$ , which represents the input current. This is left out because it is dependent on the stimulus the neuron receives, and is thus variable. Using these parameter values, we were able to generate solutions to the model in response to various stimuli (input currents). This will allow us to analyze the behavior of the system under various settings and we can observe if it exhibits the expected behavior.



### Step-Current Stimulus: 10 mV for 50 ms

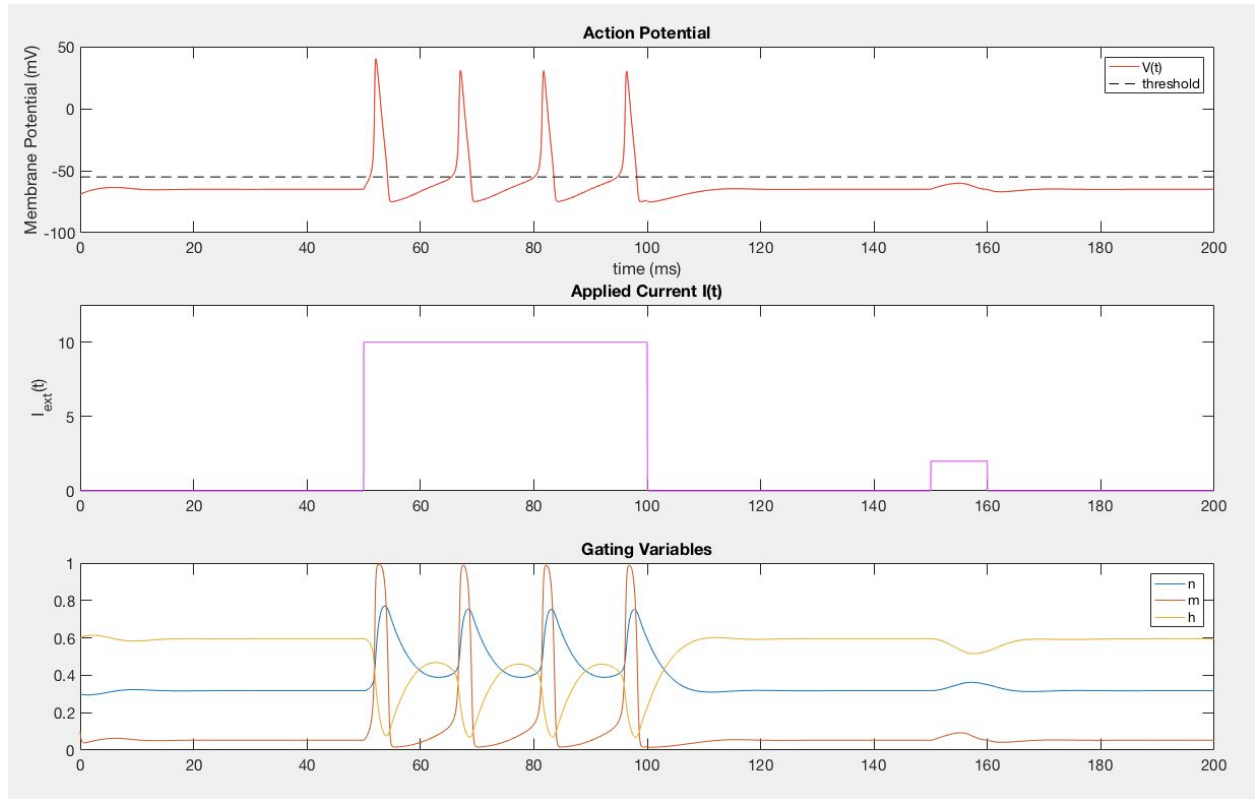


**Fig 5**

In the above figure, we see a plot of the membrane potential (top), input current (middle), and the gating variables (bottom) over time. As expected, we can see that a strong and sustained stimulus will trigger a spike in membrane potential -- *the action potential*. Furthermore, we can see that weak, transient signals do not significantly disturb the membrane potential, which soon returns to resting after the signal is gone. This reaction threshold protects the neuron from signaling pre-maturely. Random electrical noise can generate small perturbations in the membrane potential, and it can be dangerous if the cell cannot differentiate between this noise and an actual stimulus: it is hard to pass on information if you are always firing.

Note that despite the constant signal with the first step current, there is still a delay between each spike in voltage. In the biological system, this is important because it prevents the neuron from over signaling or overstimulation. Furthermore, this delay prevents a signal from traveling back down the neuron in the reverse direction [3]. These results match our expectations for a biological neuron, and gives us some confidence in the model under these settings. Mathematically, we can attribute this last result to  $h$  which is related to the  $Na^+$  inactivation gate. We see that immediately following an increase in voltage,  $h$  quickly begins to drop and is slow to recover. Due to this slow recovery, permeability to  $Na^+$  remains low following an action potential, regardless of the input current or the proportion of  $Na^+$  activation gates open. This prevents another spike in voltage until  $h$  recovers.

To illustrate the benefit of this threshold discussed earlier, we have produced a plot below (Figure 6) analyzing the results of the Hodgkin-Huxley model in the presence of zero-mean random noise (random input current).

### Random Noise ( $I_{\text{ext}}$ in $[-5,5]$ )

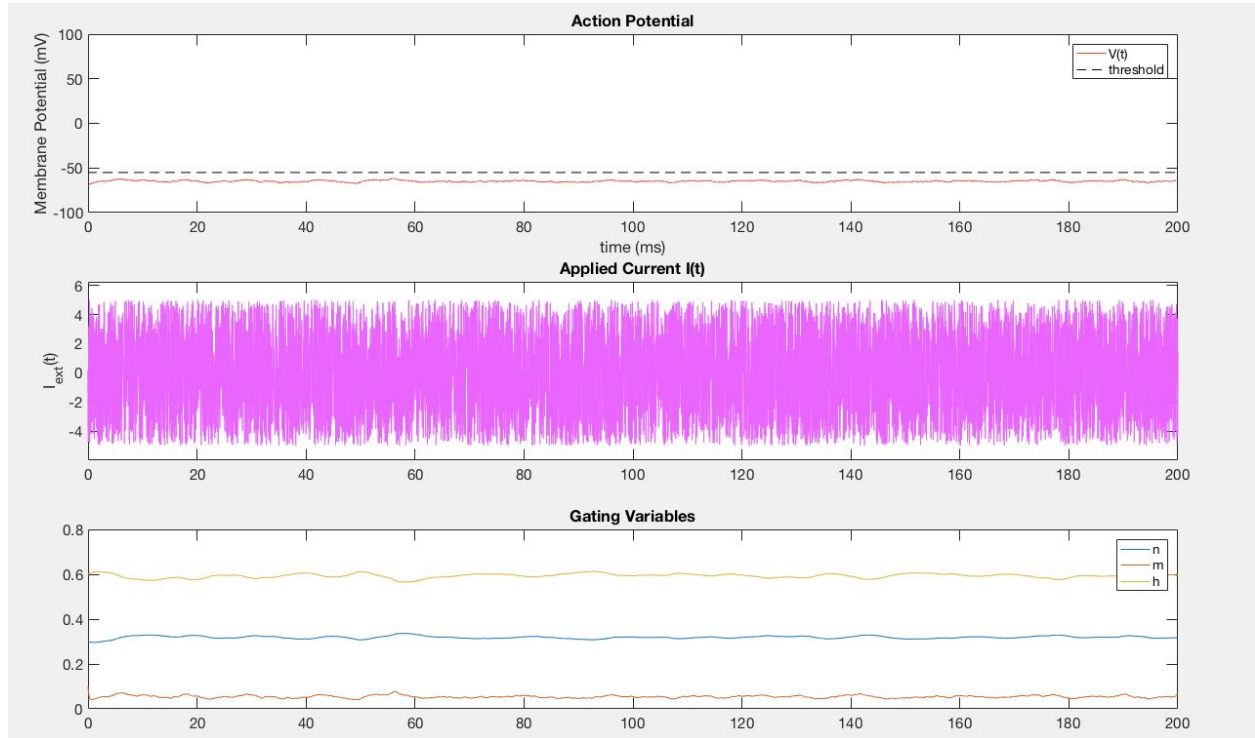


**Figure 6**

Despite significant variations in the input current, the membrane potential changes very little and there are no observed firing events. It is the presence of this apparent threshold and the oscillatory behavior of the solutions which make the Hodgkin-Huxley model a suitable model for this system.

## Mathematical Model: Fitzhugh-Nagumo Model

While the Hodgkin-Huxley model is certainly versatile, its complexity makes it difficult to analyze solutions analytically. As a result, we will motivate a further simplification of this model: the FitzHugh-Nagumo model. This model is justified by the observation that both  $V(t)$  as well as  $m(t)$  evolve on a similar time scale during an action potential--a brief spike followed by a drawn-out recovery period--while  $h(t)$  and  $n(t)$  change on much slower time scales [5] (see figure 5). Given the similarity between  $V$  and  $m$  allows us to combine them into a single variable,  $V(t)$ . The same observation can be made for  $n$  and  $1-h$ . Again we can combine both into a single

variable  $W$ , which characterize the degree of “refractoriness” of the system. The behavior of this two-dimensional system is qualitatively similar to the four-dimensional HH model [5]. This model is described below:

$$\frac{dV}{dt} = V - \frac{V^3}{3} - W + I$$

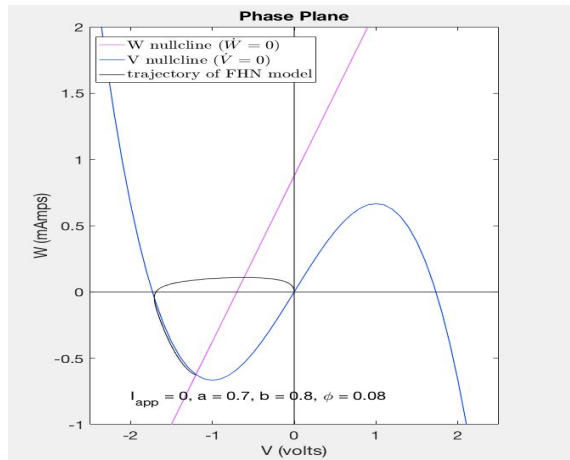
$$\frac{dW}{dt} = \phi(V + a - bW)$$

**Eqn 11** [5, pg 4]

Here,  $V$  is the voltage across the membrane and  $W$  is a recovery variable related to the refractory period following an action potential. All parameters ( $a, b, \phi$ ) are dimensionless and positive,  $\phi = 1/\tau$  and it determines how fast  $W$  changes relative to  $V$ , and  $I$  is the input current. The main goal of this simplification is to condense the *4-dimensional* Hodgkin-Huxley model down to a *2-dimensional* system which we can perform further analysis on. However, in doing so we would like to maintain the significant properties of a system: the model must generate spikes and exhibit some sort of threshold to stimulus.

## Solution of the mathematical problem

As this system is only 2-dimensional with 3 parameters ( $\phi, b, a$ ) and a variable stimulus  $I$ , we can analyze it for fixed points and attempt to quantify them. We notice the first differential equation is cubic with respect to  $V$  while the second is linear with respect to  $V$ , creating cubic and linear nullcline respectively. Below is an example of one of these such plots with a fairly standard parameter set ( $a = 0.7, b = 0.8, \phi = 0.08$ , and  $I = 0$ ). This analysis uses the file *FHN\_phase\_plane.m*.



$$V \text{ nullcline } (\dot{V} = 0) \\ W = I + V - \frac{V^3}{3}$$

$$W \text{ nullcline } (\dot{W} = 0) \\ W = \frac{V+a}{b}$$

**Fig 7**

### Finding Fixed Points of Fitzhugh-Nagumo model (FHN)

To find a fixed point of this system, we simply have to find the intersection point of these nullclines. This intersection represents a point where both  $\frac{dV}{dt}$  and  $\frac{dW}{dt}$  are zero, and is thus a fixed point. Setting the two nullcline equations equal to each other, we find that any such fixed points will satisfy:

$$\begin{aligned} \frac{b}{3}(V^*)^3 + (1 - b)V^* + (a - Ib) &= 0 \\ W^* &= \frac{V^* + a}{b} \end{aligned} \quad \text{Eqn 11}$$

As this first equation is a cubic, we are guaranteed at least 1 real root. Thus, there must be at least 1 fixed point of the system. In fact, we can prove this is the only fixed point under most standard parameter values. Firstly, note that the cubic term is always positive as  $b > 0$ . The linear term is positive iff  $b < 1$  and the constant term can be either positive or negative depending on the value of the other parameters. Applying Descartes' rule of sign, we can analyze the possible number of fixed points we may have.

If  $b > 1$ , there is a sign change between the cubic and linear term. Furthermore, there will be a sign change between the linear and constant term (it either occurs in  $f(x)$  if  $a - Ib > 0$  or in  $f(-x)$  if  $a - Ib < 0$ ). Thus, under these conditions the cubic might have three real roots, or one.

If  $b \leq 1$ , then there is no sign change between the cubic and linear term. Thus the only sign change occurs between the linear term and the constant term (it either occurs in  $f(x)$  if  $a - Ib < 0$  or in  $f(-x)$  if  $a - Ib > 0$ ) and thus there can only be a single real root. Thus, under these conditions, the fixed point is unique.

Solving for the existence of these fixed points analytically requires the cubic formula, which can be quite involved. Thus, it is difficult to analyze the existence of these fixed points due to the complexity of this formula. Rather, we can solve for the fixed points under given conditions using numerical methods.

### Stability of Fixed Points

We can assess the stability of these points by linearizing about the fixed point, and searching for the appropriate eigenvalues. First, define  $x = V - V^*$  and  $y = W - W^*$ . Using the Jacobian, this yields:

$$\begin{aligned}\frac{d}{dt} \begin{pmatrix} x \\ y \end{pmatrix} &= J_f(V^*, W^*) \begin{pmatrix} x \\ y \end{pmatrix} \\ J_f(V^*, W^*) &= \begin{pmatrix} 1 - (V^*)^2 & -1 \\ \phi & -b\phi \end{pmatrix}\end{aligned}\quad \text{Eqn 12}$$

Then to check the stability we need to check the sign of the eigenvalues of  $J_f$

$$\begin{aligned}det(J_f - \lambda I) &= (1 - (V^*)^2 - \lambda)(-b\phi - \lambda) + \phi = 0 \\ \lambda^2 + (-1 + (V^*)^2 + b\phi)\lambda + (-b\phi + b\phi(V^*)^2 + \phi) \\ \lambda &= \frac{1}{2} \left( -((V^*)^2 - 1 + b\phi) \pm \sqrt{((V^*)^2 - 1 + b\phi)^2 - 4(-b\phi + b\phi(V^*)^2 + \phi)} \right)\end{aligned}$$

We see that the eigenvalues can both be negative only if  $-b\phi + b\phi V^{*2} + \phi > 0$  (so that the root produces something less than  $V^{*2} - 1 + b\phi$ ). This occurs when  $V^{*2} > 1 - \frac{1}{b}$  or more specifically  $V^* > \sqrt{1 - \frac{1}{b}}$ ,  $V^* < -\sqrt{1 - \frac{1}{b}}$ . Furthermore,  $-(V^{*2} - 1 + b\phi)$  must also be negative. This implies  $V^{*2} > 1 - b\phi$ . As  $\phi$  is often quite small, this second condition is often the more influential one except for larger values of  $b$  (around  $b > 4$ ).

Note, that both  $1 - b\phi$  and  $1 - \frac{1}{b}$  are less than 1, as  $b$  and  $\phi$  are positive constants by definition. Solving for the maxima of the  $V$ -nullcline by taking the derivative with respect to  $V$  and setting it equal to zero, we can see that these maxima always occur at  $V = \pm 1$  regardless of the parameter values or input current. This tells us that any fixed point who exists on the left or right branches of the cubic must be stable, as  $V^{*2} > 1 > 1 - b\phi$  and  $1 - \frac{1}{b}$ . Depending on the parameters, fixed points on the central branch may or may not be stable, but those close to zero are likely unstable/saddles.

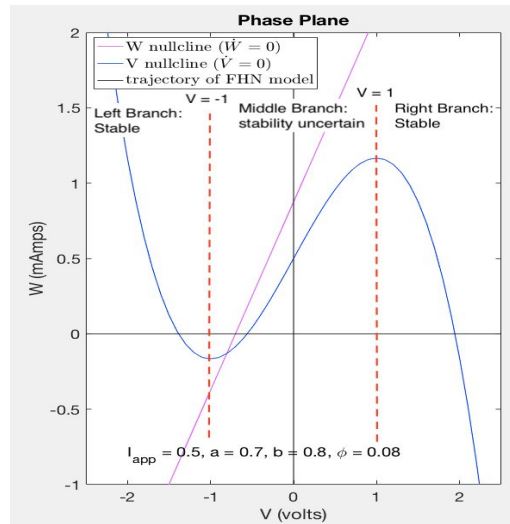


Fig 8

This last observation tells us that for the case where there are three real fixed points, there is certainly two stable fixed points and the third fixed point is likely unstable or a saddle. The reason for this is that in order to have three intersections between the cubic and linear nullcline, there must be an intersection point in each branch of the cubic. The intersections on the left and right branches will create stable fixed points as discussed earlier. For the intersection on the central branch to create a stable fixed point, it must intersect the cubic such that  $V^{*2}$  is between 1 and  $\max(1 - b\phi, 1 - \frac{1}{b})$ . In order, to intersect the cubic close to 1, the W-nullcline will have to be quite flat. Otherwise, it will not be able to intersect the other branches. As the slope of the W-nullcline depends solely on  $\frac{1}{b}$ , to flatten this line we will have to increase b. However, by increasing b, we likely expand  $\max(1 - b\phi, 1 - \frac{1}{b})$ , the frontier of instability. As a result, it seems unlikely that the central intersection can create a stable fixed point. Thus, if there is three fixed points it seems likely that the system is bistable. Our computational results below support this.

```
Jf_eigenvalues =
    -0.4174
    -0.4708

Jf_eigenvalues =
    0.8808
    -0.0831

Jf_eigenvalues =
    -0.1947 - 0.2807i
    -0.1947 + 0.2807i

fixed_points =
    -1.3146    -0.3073
     0.2058     0.4529
     1.1088     0.9044

stability =
3x1 string array
    "stable node"
    "saddle"
    "stable spiral"
```

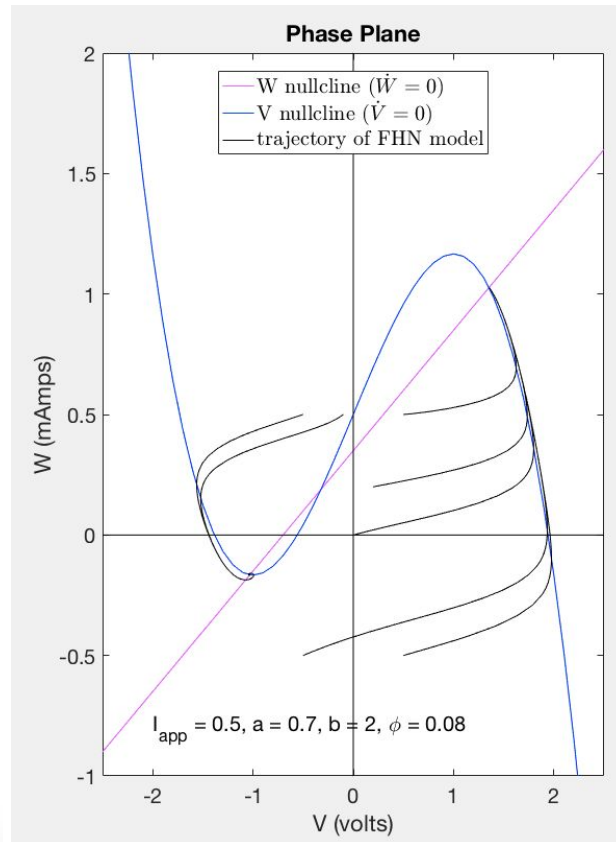


**Fig 9**

Below, we can also see that fixed points in the left and right branches exhibit the expected stable behavior. Curiously, one is a spiral and the other is a node. This may have to do with a difference in their relative proximity to a bifurcation point.

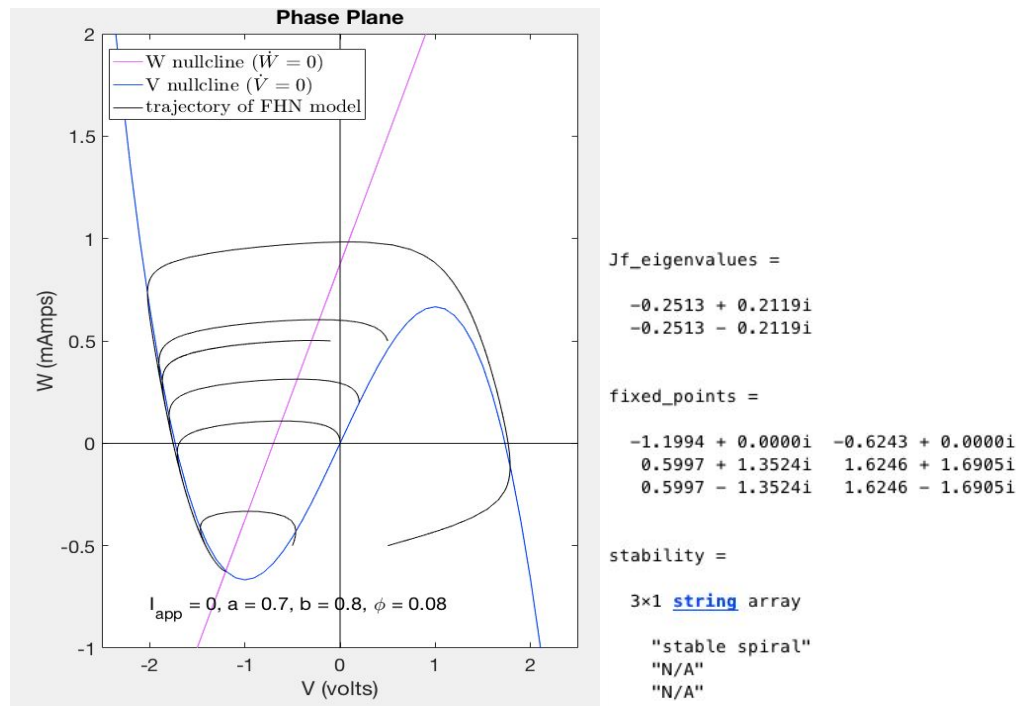


Fig 10

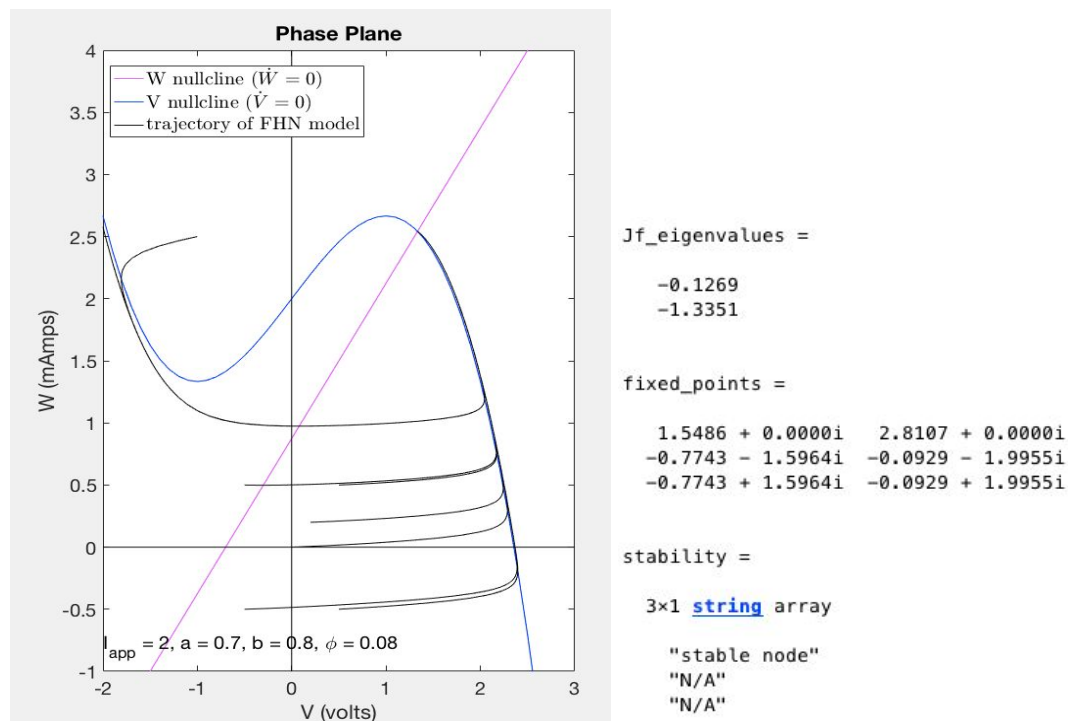
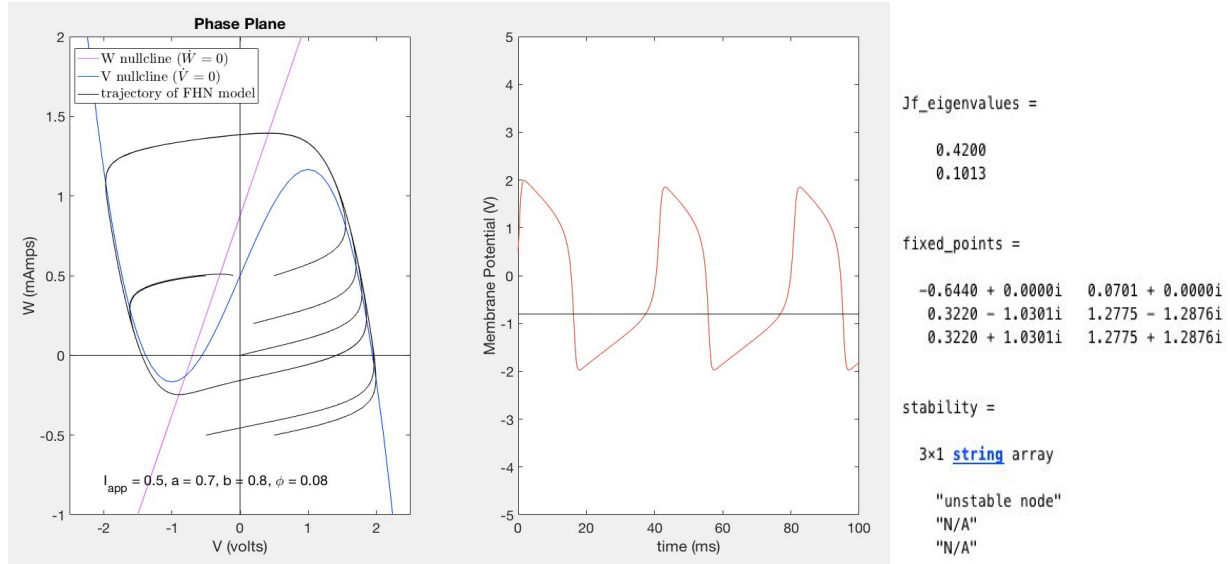


Fig 11



Under the conditions we have examined so far, we have not seen any evidence of the oscillatory behavior we expect out of an excitable system such as the neuron. To get this kind of behavior, we will examine the case where the sole fixed point is within the central branch. Note that the input current  $I_{app}$  acts as a vertical shift in the V-Nullcline, so we can change which branch the intersection between the nullclines occurs just by adjusting  $I_{app}$ . Below is an example of such a situation, using  $I_{app} = 0.5$ .



**Fig 12**

This limit cycle provides the oscillatory behavior we expected out of a model for a neuron. We notice it is stable as all trajectories flow into the limit cycle. Furthermore, as  $I_{app}$  has a significant amount of control over the fixed point, it seems we can generate systems that create such limit cycles simply by varying  $I_{app}$ . At low values of  $I_{app}$ , we saw this oscillation did not exist, but as we increased  $I_{app}$  the behavior emerged. This resembles the idea of a threshold found in biological neurons, which is a key benefit of this model. In the file *FHN\_limit\_cycle\_animation.m*, there is a script to run an animation of this system's behavior. In this animation, we can see under the standard parameter set ( $a = 0.7, b = 0.8, \phi = 0.08$ ) limit cycles emerge first when  $I_{app} \approx 0.3$  and disappear again when  $I_{app} \approx 1.35$ . See the animation for a more detailed visual of this behavior.

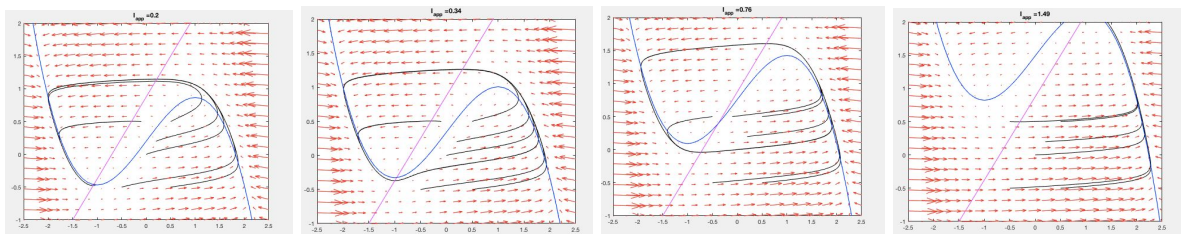


**Fig 13**



Proving such limit cycles exist in general would require the following theorem.

**Poincare-Bendixson Theorem** Suppose  $R$  is the finite region of the plane lying between two simple closed curves  $D_1$  and  $D_2$ , and  $\mathbf{F}$  is the velocity vector field for the system (1). If

(i) at each point of  $D_1$  and  $D_2$ , the field  $\mathbf{F}$  points toward the interior of  $R$ , and

(ii)  $R$  contains no critical points,

then the system (1) has a closed trajectory lying inside  $R$ .

$D_1$  could simply be chosen to be a large rectangle that surrounds the whole system, as  $\frac{dW}{dt} < 0$  anywhere to the left of the  $W$ -nullcline and greater than zero to the right, and  $\frac{dV}{dt} < 0$  anywhere above the  $V$ -nullcline and greater than zero below. Thus a rectangle containing the fixed point whose top is above and bottom below the  $V$ -nullcline, and whose sides are on opposite sides of the  $W$ -nullcline will have all vectors of the field pointing in along the boundary. However, finding  $D_2$  is more involved. For the inner curve  $D_2$ , we would have to find a curve that encloses the fixed point such that at each point of  $D_2$ , the dot product of the outward facing normal of  $D_2$  with the vector field is positive (the vector field points out of the region enclosed by  $D_2$ ; see Fig 14 below)[7]. We will leave this task for another paper.

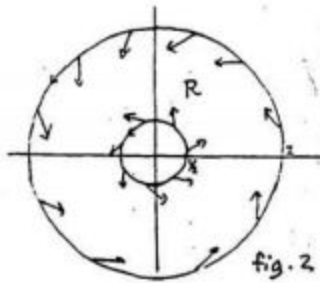


Fig 14 [7]

## Conclusion

We have motivated two models for the electrical response of a neuron: the Hodgkin-Huxley model and the Fitzhugh-Nagumo model. We simplified the behavior of the biological neuron by forming an analogy between the biological system and an electrical circuit. In doing so, we were able to apply some of the well understood properties of electrical circuits to justify our model. Additionally, we motivated a further simplification to justify the Fitzhugh Nagumo model, recognizing the similarity in behavior between several variables in the Hodgkin-Huxley model. Computationally, we were able to verify both systems exhibit the general desired behavior of the biological system: an apparent threshold and oscillatory behavior.

With the Fitzhugh-Nagumo model, we were able find fixed points of the system, although solving for them explicitly required the cubic formula. Generally, we were able to

discuss the existence of these fixed points and assess their stability based on where the nullcline intersected on the cubic. We found that the outer branches of the cubic created stable fixed points, while oscillatory behavior was sometimes generated within the middle branch. We analyzed the existence of these limit cycles under the standard parameter values, and found that it varies with the input current.

Both models present reasonable analogs of the excitable behavior found within a neuron. However, both have their drawbacks as well. The Fitzhugh-Nagumo model loses its limit cycles if  $I_{app}$  increases too much, which is uncharacteristic of a biological system. Also, both models are limited in their ability to integrate stimuli coming from multiple sources.

In a future paper, we would like to prove generally the existence of these limit cycles under the standard parameter set, which would require finding a suitable trapping region. Furthermore, we would like to explore the apparent bifurcations of the system.

## References

- [1] Ermentrout, Bard, and David H. Terman. *Foundations of Mathematical Neuroscience*. (2010).
- [2] A.L. Hodgkin, A.F. Huxley. A Quantitative Description of Membrane Current and its Application to Conduction and Excitation in Nerve. *Journal of Physiology* (117). (1952),
- [3] Peter Dayan, L.F. Abbott. *Theoretical Neuroscience: Computational and Mathematical Modeling of Neural Systems*. (2005).
- [4] F. Buchholtz, N. Schinor, and, and F. W. Schneider\*, Stochastic Nonlinear Dynamics: How Many Ion Channels are in a Single Neuron?, *The Journal of Physical Chemistry B* 2002 106 (19), 5086-5090
- [5] Hodgkin-Huxley Theory of Nerve Membranes: The FitzHugh-Nagumo model, <https://www.ugr.es/~jtorres/FNtema7.pdf>
- [6] Ermentrout, G. Bard, Terman, David H. The Hodgkin-Huxley equations. (2010)
- [7] Mattuck, Arthur. Ordinary Differential Equations 18.03 Notes and Exercises: Limit cycles. <https://math.mit.edu/~jorloff/supnnotes/supnnotes03/lc.pdf>

## Picture Sources

- Action potential spreading down axon (Fig 2a)
  - Propagation of action potential, <http://physiologyplus.com/propagationconduction-of-action-potential/>
- Interior of axon image (Fig 1)
  - Action potential, <http://ib.bioninja.com.au/standard-level/topic-6-human-physiology/65-neurons-and-synapses/action-potential.html>
- Action potential graph (Fig 2b)
  - [https://www.researchgate.net/figure/Diagram-for-action-potential\\_220048032](https://www.researchgate.net/figure/Diagram-for-action-potential_220048032)

